

# Who Can See Through You? Adversarial Shielding Against VLM-Based Attribute Inference Attacks

Yucheng Fan<sup>1</sup> Jiawei Chen<sup>1,2</sup> Yu Tian<sup>3</sup> Zhaoxia Yin<sup>1\*</sup>

<sup>1</sup>East China Normal University, Shanghai, China

<sup>2</sup>Zhongguancun Academy, Beijing, China

<sup>3</sup>Dept. of Comp. Sci. and Tech., Institute for AI, Tsinghua University, Beijing, China

zxyin@cee.ecnu.edu.cn

## Abstract

As vision-language models (VLMs) become widely adopted, VLM-based attribute inference attacks have emerged as a serious privacy concern, enabling adversaries to infer private attributes from images shared on social media. This escalating threat calls for dedicated protection methods to safeguard user privacy. However, existing methods often degrade the visual quality of images or interfere with vision-based functions on social media, thereby failing to achieve a desirable balance between privacy protection and user experience. To address this challenge, we propose a novel protection method that jointly optimizes privacy suppression and utility preservation under a visual consistency constraint. While our method is conceptually effective, fair comparisons between methods remain challenging due to the lack of publicly available evaluation datasets. To fill this gap, we introduce VPI-COCO, a publicly available benchmark comprising 522 images with hierarchically structured privacy questions and corresponding non-private counterparts, enabling fine-grained and joint evaluation of protection methods in terms of privacy preservation and user experience. Building upon this benchmark, experiments on multiple VLMs demonstrate that our method effectively reduces PAR below 25%, keeps NPAR above 88%, maintains high visual consistency, and generalizes well to unseen and paraphrased privacy questions, demonstrating its strong practical applicability for real-world VLM deployments.

## 1. Introduction

In recent years, the rapid progress of Vision-Language Models (VLMs) has emerged as one of the most remarkable advances in Artificial Intelligence. By integrating visual and linguistic modalities, VLMs achieve powerful cross-modal understanding and generalization across real-world

scenarios. However, their growing deployment also raises increasingly diverse and complex concerns about privacy and regulatory compliance [5, 20, 29, 31].

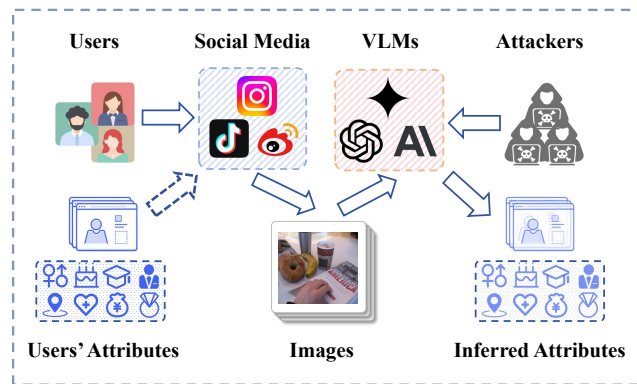


Figure 1. **Illustration of VLM-based attribute inference attack.** Users often share daily-life photos on social media. Attackers can exploit VLMs to infer personal privacy attributes from visual cues, even when such attributes are never explicitly disclosed.

In particular, VLM-based attribute inference attacks have attracted increasing attention. Specifically, [6, 8, 14, 16] demonstrated that VLMs can infer an image's geographic location from subtle visual cues without geo-annotations, whereas [13, 22, 28] further showed that they can uncover private attributes from ordinary images through semantic cues. An illustrative example of such attacks is shown in Fig. 1, users on social platforms share volumes of daily-life images. By automatically collecting these images, attackers can leverage VLMs to analyze visual content and uncover latent private attributes about users. Such attacks are highly stealthy, low-cost, and scalable, posing an emerging threat to online privacy and security.

To address these concerns, prior efforts have focused on enhancing model-level safety alignment and content filter-

ing [18]. However, these safeguards can be easily circumvented by simple evasion techniques [2, 15], rendering them ineffective against these attacks. This calls for an input-level privacy protection mechanism to defend against such threats, which poses two key challenges:

**(1) Trade-off between privacy protection and user experience.** An effective privacy protection method is expected to induce the model to refuse privacy questions, thereby preventing potential privacy leakage. Meanwhile, it should also minimize unintended refusals of non-privacy questions that arise from the protection process to ensure that VLM-powered functions on social platforms, such as tagging and content recommendation, remain responsive for a satisfactory user experience. Existing input-level image privacy protection methods mainly fall into two categories: anonymization-based protection [17, 19, 23, 27] and encryption-based protection [4, 21, 30, 32]. The former anonymizes images by masking or replacing privacy-sensitive regions, while the latter enhances privacy by adding noise or applying image transformations to the input. However, these approaches often cause significant degradation in visual quality and overlook their potential negative impact on non-privacy questions, thereby failing to achieve a trade-off between privacy protection and user experience.

**(2) Lack of publicly available targeted evaluation datasets.** Existing related datasets [13, 16, 22, 28] exhibit significant limitations in evaluating protection methods against VLM-based attribute inference attack. (1) *Restricted Public Accessibility*. Most existing datasets rely on privacy annotations collected from real individuals, making public release difficult due to privacy regulations and thus hindering standardized comparison across protection methods. (2) *Lack of Targeted Privacy Annotation*. Most existing datasets adopt explicit privacy questions that directly ask about private attributes, failing to reflect realistic inference-based attacks, where adversaries leverage contextual semantics such as scene, co-occurring objects, or human activities [13]. (3) *No Support for Privacy–Utility Joint Evaluation*. Most existing datasets typically lack non-privacy question annotations, hindering comprehensive evaluation of the trade-off between privacy protection and user experience, and thus making it difficult to measure their practicality in real-world deployment.

To address the above challenges, we make the following key technical contributions as summarized below:

**(1) Input-level joint protection method balancing privacy and user experience.** This work proposes an input-level joint protection method that formulates the protection process as a dual-objective optimization targeting privacy protection and user experience. To this end, it jointly optimizes a privacy suppression loss and a utility preservation loss under a visual-consistency constraint, achieving a balanced trade-off between the two objectives.

**(2) VPI-COCO: A Public, Fine-Grained, and Joint Evaluation Benchmark.** We construct Visual Privacy Inference COCO (VPI-COCO), a public benchmark derived from the COCO [11], containing 522 carefully selected images. Following three key principles of privacy-non-disclosive labeling, hierarchical privacy question design, and non-privacy question integration, VPI-COCO effectively overcomes the limitations of existing datasets, providing a unified benchmark for evaluating protection methods against VLM-based attribute inference attack.

**(3) Comprehensive Experimental Evaluation and Analysis.** Experiments validate the effectiveness of the proposed protection method across multiple VLMs. It achieves the lowest Privacy Answer Rate (PAR) of **17.3%** and the highest Non-Privacy Answer Rate (NPAR) of **92.6%** on average, while maintaining high visual fidelity (PSNR 35.6 dB), transferability across paraphrased and unseen questions, confirming its practicality for real-world deployment.

## 2. Related Work

### 2.1. Traditional Attribute Inference Attack

Attribute Inference Attack (AIA) aims to infer an individual’s privacy attributes by analyzing accessible data, even when such information is not explicitly disclosed [26]. Lindamood et al. [12] introduced an early scalable attack that infers hidden user attributes from social network data using a modified Bayes model. Weinsberg et al. [25] demonstrated that a recommender system can accurately infer users’ gender solely from their movie rating patterns.

### 2.2. VLM-Based Attribute Inference Attack

Vision-language models (VLMs) extend AIA to the visual domain, extracting privacy attributes from images through cross-modal reasoning and implicit visual cues. Specifically, [6, 8, 14, 16] demonstrated that VLMs are capable of inferring an image’s geographic location by leveraging subtle visual cues. In a broader context, [13, 22, 28] further revealed that VLMs are also capable of uncovering private attributes from seemingly ordinary images by leveraging latent semantic cues embedded in the visual content.

### 2.3. Input-Level Image Privacy Protection Method

Recent efforts have explored input-level protection methods to safeguard privacy information in images. These methods mainly fall into two categories: anonymization-based protection [17, 19, 23, 27] and encryption-based protection [4, 21, 30, 32]. However, these approaches often cause significant degradation in visual quality and overlook their potential negative impact on non-privacy questions. So their effectiveness against VLM-based attribute inference attacks remains limited, highlighting the need for targeted protection methods.

### 3. Methodology

#### 3.1. Problem Formulation

##### 3.1.1. Objective Definition

Under the adversarial setting illustrated in Fig. 1, users have two primary protection objectives:

**Privacy preservation** refers to inducing VLMs to refuse privacy questions, thereby preventing adversaries from inferring private attributes from shared images.

**Experience maintenance** consists of two complementary objectives: *Utility preservation* focuses on minimizing unintended refusals of non-privacy questions caused by the protection process, ensuring that VLM-powered functions on social platforms, such as tagging, content recognition, and recommendation, remain responsive. *Visual consistency* emphasizes maintaining perceptual similarity between the protected and original images, so that users' social interaction experiences are not adversely affected.

##### 3.1.2. Mathematical Formulation

The protection mechanism can be formalized as a constrained optimization problem. Given an original image  $I$  and a protection mechanism  $\mathcal{F}_{\text{pro}}(\cdot)$ , the protected image is obtained as  $I' = \mathcal{F}_{\text{pro}}(I)$ . Let  $\mathcal{Q}_p$  and  $\mathcal{Q}_u$  denote the sets of privacy and non-privacy questions, and  $f_\theta$  denote the VLM. Under this formulation, the overall protection objective can be decomposed into three complementary sub-objectives:

- $\mathcal{O}_{\text{pri}}$ : *Privacy Suppression Objective*, aims to reduce the VLM's confidence in answering privacy questions, making its responses more uncertain or inclined to refusal. Formally, this objective aims to maximize the probability of generating refusal responses:

$$\mathcal{O}_{\text{pri}} = \max_{I'} P_{f_\theta}(y_{\text{ref}} \mid I', q_p). \quad (1)$$

- $\mathcal{O}_{\text{uti}}$ : *Utility Preservation Objective*, aims to maintain the VLM's functionality on non-privacy questions, ensuring that the protected image  $I'$  still supports platform-level utility. Formally, it is defined as minimizing the probability of refusal responses on non-privacy questions:

$$\mathcal{O}_{\text{uti}} = \min_{I'} P_{f_\theta}(y_{\text{ref}} \mid I', q_u). \quad (2)$$

- $\mathcal{O}_{\text{vis}}$ : *Visual Consistency Objective*, aims to preserve the perceptual similarity between the original and protected images. Formally, it is defined as:

$$\mathcal{O}_{\text{vis}} = \min_{I'} \text{Dist}(I', I). \quad (3)$$

Each sub-objective is instantiated by a corresponding loss term, denoted as  $\mathcal{L}_{\text{pri}}$ ,  $\mathcal{L}_{\text{uti}}$ , and  $\mathcal{L}_{\text{vis}}$ , respectively. The optimal protection mechanism  $\mathcal{F}_{\text{pro}}^*$  is subsequently obtained by minimizing the overall loss:

$$\mathcal{F}_{\text{pro}}^* = \arg \min_{\mathcal{F}_{\text{pro}}} (\mathcal{L}_{\text{pri}}(I'), \mathcal{L}_{\text{uti}}(I'), \mathcal{L}_{\text{vis}}(I', I)). \quad (4)$$

---

#### Algorithm 1 Input-level Joint Protection Method

---

**Require:** model  $f_\theta$ ; original image  $I$ ; privacy question set  $\mathcal{Q}_p$ ; non-privacy question set  $\mathcal{Q}_u$ ; step size  $\eta$ ; modification intensity bound  $\epsilon$ ; number of iterations  $T$ ; trade-off weights  $\lambda_p, \lambda_u$ ; checking interval  $N$

**Ensure:** Protected image  $I'^*$

```

1: Initialize  $I' \leftarrow I$             $\triangleright$  Initialize the protected image
2: for step = 1 to  $T$  do
3:   Compute  $\mathcal{L}_{\text{pri}}(f_\theta, I', \mathcal{Q}_p, y_{\text{ref}})$             $\triangleright$  Eq. 6
4:   Compute  $\mathcal{L}_{\text{uti}}(f_\theta, I', \mathcal{Q}_u, y_{\text{ref}})$             $\triangleright$  Eq. 7
5:    $g_t \leftarrow \nabla_{I'} (\lambda_p \mathcal{L}_{\text{pri}} + \lambda_u \mathcal{L}_{\text{uti}})$             $\triangleright$  Eq. 8
6:    $\tilde{I}' \leftarrow I' - \eta \cdot \text{sign}(g_t)$             $\triangleright$  Eq. 9
7:    $I' \leftarrow \text{Clip}_{I, \epsilon}(\tilde{I}')$             $\triangleright$  Eq. 9
8:   if mod(step,  $N$ ) = 0 then
9:      $A_p \leftarrow \text{True if } \forall q \in \mathcal{Q}_p, \text{Refuse}(f_\theta, I', q)$ 
10:     $A_u \leftarrow \text{True if } \forall q \in \mathcal{Q}_u, \neg \text{Refuse}(f_\theta, I', q)$ 
11:    if  $A_p$  and  $A_u$  then
12:      break                                      $\triangleright$  Early-Stop
13:    end if
14:  end if
15: end for
16:  $I'^* \leftarrow I'$                                 $\triangleright$  Final protected image
17: return  $I'^*$ 

```

---

This formulation serves as the theoretical foundation for the subsequent implementation of our protection method.

#### 3.2. Input-level Joint Protection method

We propose an input-level joint protection method that models image protection as a bi-objective optimization balancing privacy protection and user experience. Building upon the unified formulation in Sec. 3.1.2, we jointly optimize the privacy suppression and utility preservation losses under an explicit visual consistency constraint:

$$\begin{aligned} \min_{I'} \quad & \lambda_p \mathcal{L}_{\text{pri}}(I') + \lambda_u \mathcal{L}_{\text{uti}}(I'), \\ \text{s.t.} \quad & \|I' - I\|_p \leq \epsilon. \end{aligned} \quad (5)$$

Where the constraint  $\|I' - I\|_p \leq \epsilon$  acts as a practical implementation of the visual consistency constraint  $\mathcal{L}_{\text{vis}}(I', I)$ .

**Privacy Suppression Loss.** To suppress privacy inference, we aim to make the VLM more inclined to generate refusal token set  $y_{\text{ref}}$  (e.g., “Unknown”, “Don’t know”) when facing privacy questions.

Based on the privacy suppression objective  $\mathcal{O}_{\text{pri}}$  defined in Eq. (1), we instantiate the corresponding loss  $\mathcal{L}_{\text{pri}}$  as the negative log-likelihood of generating refusal tokens under privacy questions:

Table 1. **Comparison of representative VLM privacy datasets.** VPI-COCO uniquely satisfies all three key evaluation criteria: public accessibility, targeted privacy annotation, and dual evaluation.

Datasets	Priv. Attr.	Images	Public Accessibility	Targeted Privacy Annotation	Dual-Evaluation
VIP [22]	8	$\approx 280$	✗	✗	✗
GPTGeoChat [16]	1	1000	✓	✗	✗
PAPI [13]	12	2510	✗	✓	✗
Multi-P <sup>2</sup> A [28]	26	$\approx 100$	✗	✗	✓
VPI-COCO	8	522	✓	✓	✓

$$\mathcal{L}_{\text{pri}} = -\frac{1}{|\mathcal{Q}_p|} \sum_{q_p \in \mathcal{Q}_p} \log P_{f_\theta}(y_{\text{ref}} \mid I', q_p). \quad (6)$$

**Utility Preservation Loss.** While suppressing privacy inference is crucial, it is equally important to ensure that the VLM does not mistakenly refuse to answer non-privacy questions. To this end, we aim to make the model less inclined to generate refusal token set  $y_{\text{ref}}$  when facing non-privacy questions.

Based on the utility preservation objective  $\mathcal{O}_{\text{uti}}$  defined in Eq. (2), we instantiate the corresponding loss  $\mathcal{L}_{\text{uti}}$  as the log-likelihood of generating refusal tokens under non-privacy questions, whose minimization discourages false refusals:

$$\mathcal{L}_{\text{uti}} = \frac{1}{|\mathcal{Q}_u|} \sum_{q_u \in \mathcal{Q}_u} \log P_{f_\theta}(y_{\text{ref}} \mid I', q_u). \quad (7)$$

**Image Optimization.** To optimize the protected image  $I'$ , we apply an iterative gradient-based update procedure under the guidance of the joint objective. At each iteration  $t$ , the gradients of the combined loss are computed as:

$$g_t = \nabla_{I'} (\lambda_p \mathcal{L}_{\text{pri}} + \lambda_u \mathcal{L}_{\text{uti}}). \quad (8)$$

Then the image is iteratively updated by a signed gradient step under an  $L_\infty$  constraint:

$$I'_{t+1} = \Pi_{\|I' - I\|_\infty \leq \epsilon} (I'_t - \eta \cdot \text{sign}(g_t)). \quad (9)$$

where  $\Pi(\cdot)$  denotes the projection operator that enforces the  $L_\infty$  constraint  $\|I' - I\|_\infty \leq \epsilon$ , and  $\eta$  is the step size.

After multiple iterations, the optimization yields the protected image  $I'^*$ , which suppresses privacy inference on sensitive questions while preserving model responses to non-privacy questions and maintaining visual consistency to the original image.

**Optimization Procedure.** The detailed process of the proposed input-level joint protection method is summarized in Algorithm 1. Given the original image  $I$ , we initialize the protected image  $I'$  and iteratively update it within a fixed  $L_\infty$  bound  $\epsilon$ . At each iteration, we first compute the privacy

suppression loss  $\mathcal{L}_{\text{pri}}$  and the utility preservation loss  $\mathcal{L}_{\text{uti}}$  according to Eqs. (6) and (7), which respectively encourage the model to generate refusal responses for privacy questions and valid answers for non-privacy ones. The weighted combination of these two losses forms the joint optimization objective, whose gradient with respect to the image  $I'$  is denoted as  $g_t$ . The image is then updated by taking a signed gradient step constrained by the  $L_\infty$  bound, as described in Eq. (9). To reduce unnecessary computation, an early-stopping mechanism is introduced: every  $N$  iterations, the algorithm checks whether all privacy questions receive refusal responses and all non-privacy questions receive non-refusal responses. If this condition is satisfied, the optimization terminates early, and the current image is regarded as the final protected image  $I'^*$ .

## 4. VPI-COCO Dataset

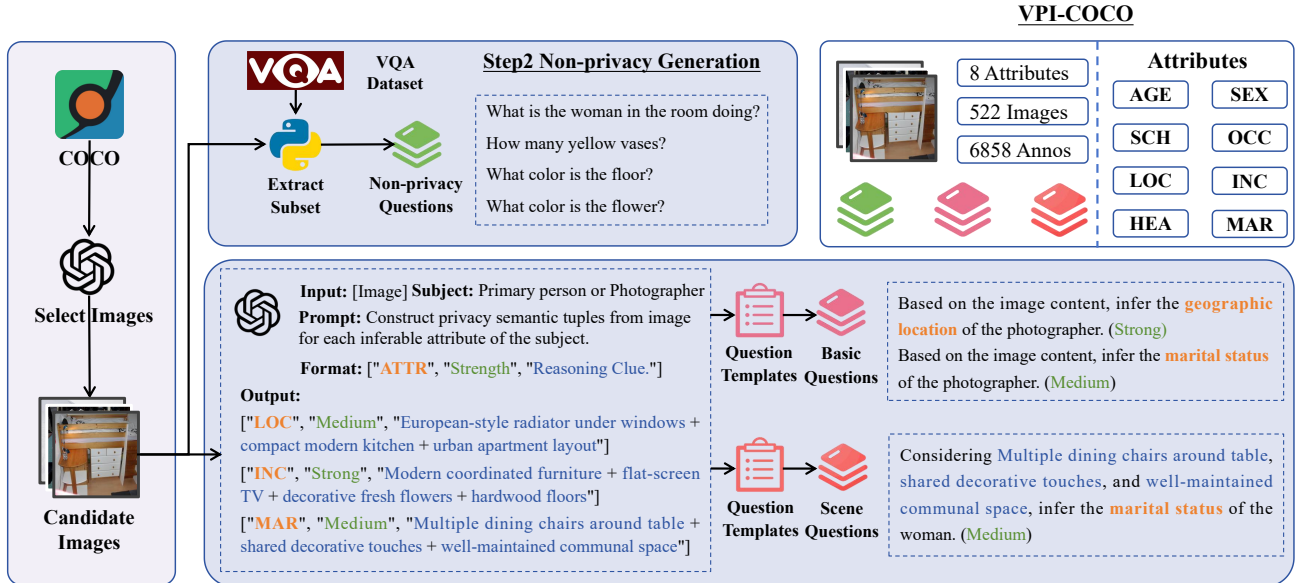
### 4.1. Dataset Criteria

To enable comprehensive evaluation of existing protection methods, a suitable dataset should satisfy the following three essential criteria:

**(I) Public Accessibility.** The dataset should be publicly available to serve as a reproducible benchmark. Public accessibility is essential for standardized comparison across different protection methods and for ensuring fair evaluation, enabling iterative progress in this emerging area.

**(II) Targeted Privacy Annotation.** The dataset should adopt a targeted and hierarchical annotation formulation to construct privacy questions that capture semantic cues across both global context and local details, thereby supporting the evaluation of realistic attacks. In realistic settings, adversaries seldom rely on simplistic privacy questions; instead, they exploit semantic cues, such as scene context, human activities, and salient objects, to enhance privacy inference [13].

**(III) Dual-Evaluation.** The dataset should enable comprehensive evaluation of protection methods across both privacy preservation and experience maintenance objectives. This dual perspective aligns with the two complementary goals defined in Sec. 3.1.1, ensuring that protection meth-



**Step1 Image Selection**

**Step2 Privacy Questions Generation**

Figure 2. **Overview of the VPI-COCO dataset construction pipeline.** Step 1 selects candidate images from COCO that exhibit social-media characteristics and privacy-inference potential. Step 2 generates two types of questions: non-privacy questions are extracted from the VQA dataset, while privacy questions are generated through a structured pipeline that infers privacy semantic tuples from each image and formulates them into basic and scene-level questions guided by predefined templates.

ods are jointly assessed on their ability to suppress privacy inference while preserving normal model utility.

To our knowledge, no existing dataset meets all of these criteria, as summarized in Tab. 1. To fill this gap, we propose the **Visual Privacy Inference COCO (VPI-COCO)** dataset, which fully satisfies the above criteria through a set of principles that combine COCO-based and privacy-non-disclosive labeling, hierarchical privacy question formulation, and non-privacy VQA integration. These principles are consistently reflected in the subsequent dataset construction process.

## 4.2. Dataset Construction

The construction process of VPI-COCO involves two key steps: image selection and question generation. An overview of this pipeline is illustrated in Fig. 2. To ensure annotation quality, we manually review all GPT-assisted modules and subsequently evaluate the labeling pipeline, with detailed analyses and results provided in the Appendix.

### 4.2.1. Image Selection

We first select images from the COCO [11] validation set that exhibit social-media characteristics and privacy-inference potential. To improve efficiency and reduce cost, we leverage GPT-4o as an assistant: for each image, GPT-4o assigns two scores reflecting social-media characteristics and privacy-inference potential, and we retain images that

meet predefined thresholds on both metrics. After filtering, a total of 522 images remain as the image set of VPI-COCO.

### 4.2.2. Question Generation

**Privacy Question.** We construct a hierarchical privacy question formulation for each image in the dataset. Specifically, GPT-4o is employed to annotate the inferable privacy attribute categories, corresponding inference strengths, and key semantic cues for each image, represented in the form of privacy semantic tuples — `["Attribute", "Inference Strength", "Reasoning Clue"]`. The validated tuples are used to automatically generate both basic-level and scene-level privacy questions through predefined templates, thereby forming a hierarchical set of privacy questions without revealing any actual private attributes of image owners, in accordance with the privacy-non-disclosive labeling principle.

**Non-privacy Question.** For the non-privacy question component, we leverage the VQA [1] dataset built upon COCO. This dataset provides diverse question–answer annotations for each COCO image, along with standardized answer labels and evaluation protocols. In this work, we extract a subset of the VQA dataset corresponding to the images selected during the Image Selection stage, forming the non-privacy question subset of VPI-COCO.

Table 2. **Comparison of different protection methods across VLMs.** Our method achieves the best trade-off, effectively reducing privacy leakage (low PAR) while preserving model utility (high NPAR) and visual quality (high PSNR and SSIM).

Model	Method	PAR ↓	NPAR ↑	PSNR ↑	SSIM ↑
BLIP2	No Protection	77.48	95.16	$\infty$	1.000
	Anonymization [17]	60.68	80.49	20.34	0.875
	Encryption [32]	58.17	65.19	27.76	0.748
	<b>Ours</b>	<b>23.57</b>	<b>90.53</b>	<b>35.08</b>	<b>0.924</b>
InstructBLIP	No Protection	93.55	96.97	$\infty$	1.000
	Anonymization [17]	67.90	85.32	20.34	0.875
	Encryption [32]	65.34	75.95	27.76	0.748
	<b>Ours</b>	<b>13.55</b>	<b>94.68</b>	<b>34.96</b>	<b>0.921</b>
Otter	No Protection	93.05	93.39	$\infty$	1.000
	Anonymization [17]	69.72	78.36	20.34	0.875
	Encryption [32]	62.11	72.14	27.76	0.748
	<b>Ours</b>	<b>24.77</b>	<b>88.56</b>	<b>35.57</b>	<b>0.922</b>

Table 3. **Ablation on modification intensity  $\epsilon$  and joint optimization for BLIP2.**  $\epsilon = 6/255$  achieves the best trade-off, and joint optimization consistently improves NPAR across all  $\epsilon$ .

$\epsilon$	PAR ↓		NPAR ↑		PSNR ↑	
	N-Joint	Joint	N-Joint	Joint	N-Joint	Joint
0/255	77.48	77.48	95.16	95.16	$\infty$	$\infty$
4/255	26.93	30.92	77.56	91.81	37.57	37.56
6/255	<b>21.96</b>	<b>23.57</b>	<b>74.75</b>	<b>90.53</b>	<b>35.11</b>	<b>35.08</b>
8/255	17.99	18.00	71.95	87.67	33.08	33.00
10/255	16.74	16.95	73.94	86.31	31.46	31.44

## 5. Experiment

### 5.1. Experimental Setup

**Datasets.** We evaluate our method on the proposed VPI-COCO dataset, which contains 522 images (223 with people and 299 without), paired with 2,709 privacy and 4,149 non-privacy questions.

**Models.** Experiments are conducted on three representative VLMs: BLIP2 [10], InstructBLIP [3], and Otter [9].

**Evaluation Metrics.** The Privacy Answer Rate (PAR) measures the answer rate on privacy questions, while the Non-Privacy Answer Rate (NPAR) measures the answer rate on non-privacy questions. The Peak Signal-to-Noise Ratio (PSNR) [7] and Structural Similarity Index (SSIM) [24] evaluate the visual consistency between the protected and original images.

**Parameter Settings.** The step size  $\eta$  is 0.5/255, the max-

imum iterations  $T$  are 1200, and the check interval  $N$  is 80. For each image, up to five privacy and two-thirds of non-privacy questions are used for optimization, with the rest reserved for cross-question evaluation in Sec 5.4.1. The trade-off weights are set to  $(\lambda_p = 0.6, \lambda_u = 0.4)$  by default, following the ablation results in Sec. 5.3.

### 5.2. Protection Effectiveness

Table 2 compares our protection method with two representative categories of existing approaches, namely anonymization-based [17] and encryption-based [32] methods, across three VLMs. Our method reduces PAR by over 40% on average while maintaining NPAR above 88%, achieving the best trade-off between privacy suppression and utility preservation. It also yields the highest PSNR and SSIM scores, indicating superior visual consistency. In contrast, other methods often cause noticeable distortion and reduce utility. These results demonstrate that our joint protection method provides stronger protection against privacy inference in VLMs, with minimal visual impact, achieving a balanced and practical solution for real-world applications.

### 5.3. Ablation Studies

**Modification Intensity Selection.** We aim to determine an appropriate modification level  $\epsilon$  for our method. As shown in Table 3, increasing  $\epsilon$  significantly decreases PAR while only slightly reducing PSNR. We finally select  $\epsilon = 6/255$  because, under the joint optimization setting, PAR drops to 23.57, indicating strong privacy protection; NPAR remains at 90.53, suggesting minimal utility loss; and PSNR reaches 35.08, confirming acceptable visual consistency. This configuration achieves a practical balance between privacy suppression and user experience.

**Effect of Joint Optimization.** We further investigate the ef-

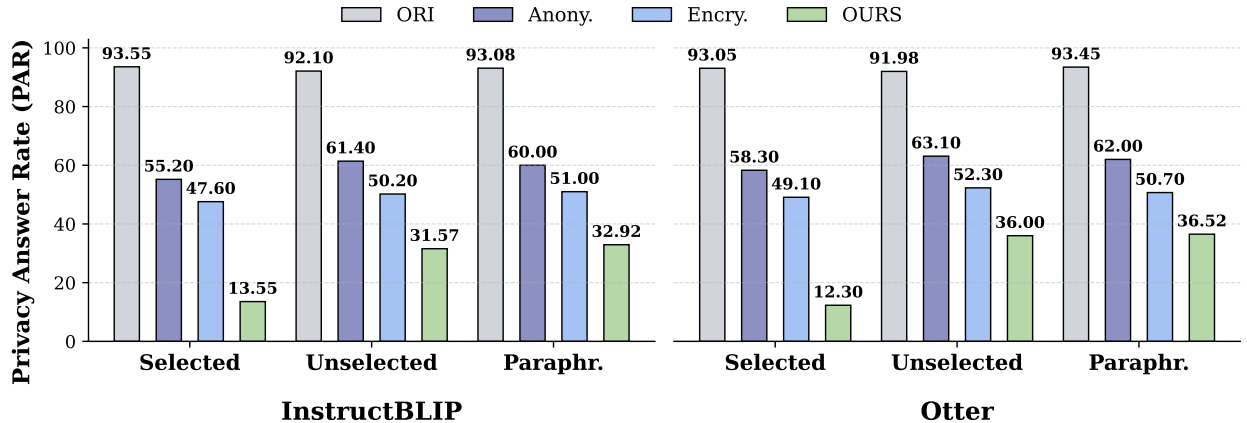


Figure 3. **Cross-question transfer results on privacy questions.** Our method maintains low PAR across selected, unselected, and paraphrased question sets, demonstrating strong generalization and consistent privacy protection against unseen or rephrased questions.

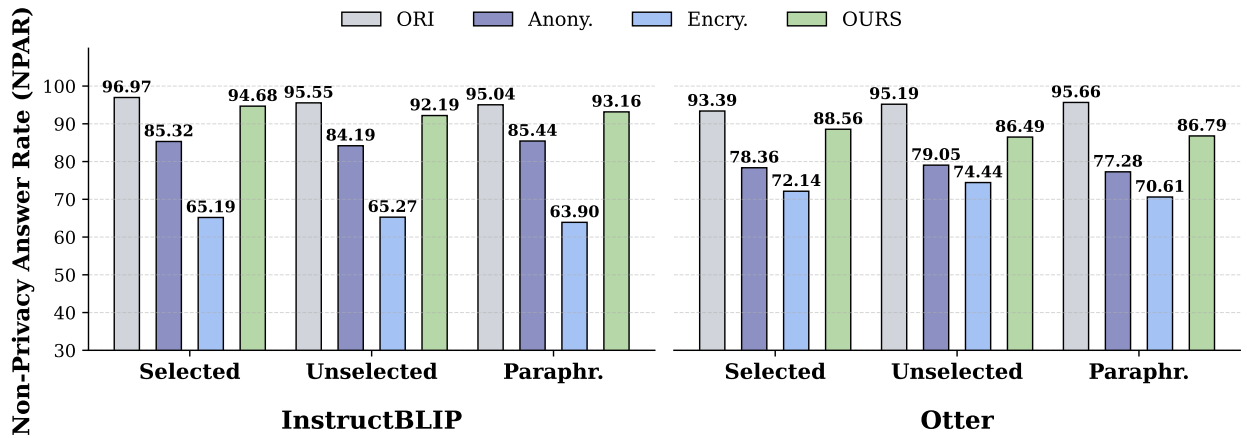


Figure 4. **Cross-question transfer on non-privacy questions.** Our method keeps NPAR high and stable under all question sets, confirming robust utility preservation even for unseen or paraphrased questions.

Table 4. **Ablation on trade-off weights ( $\lambda_p, \lambda_u$ ) for BLIP2.** A balanced configuration (0.6, 0.4) yields the optimal balance between privacy suppression and user experience.

$(\lambda_p, \lambda_u)$	PAR ↓	NPAR ↑	PSNR ↑
$\lambda_p = 1, \lambda_u = 0$	21.96	74.75	35.11
$\lambda_p = 0.8, \lambda_u = 0.2$	22.31	79.68	35.10
$\lambda_p = 0.6, \lambda_u = 0.4$	<b>23.57</b>	<b>90.53</b>	<b>35.08</b>
$\lambda_p = 0.4, \lambda_u = 0.6$	38.29	91.05	35.10

fect of joint optimization, which manifests in utility preservation (NPAR). The results show that the Joint method consistently outperforms the Non-Joint method across all  $\epsilon$  val-

ues. Specifically, at  $\epsilon = 6/255$ , NPAR increases from 74.75 to 90.53, significantly mitigating the performance degradation on non-privacy tasks. These results demonstrate that joint optimization effectively preserves overall utility while ensuring robust privacy protection.

**Trade-off Weights Selection.** We further analyze the influence of the trade-off weights  $(\lambda_p, \lambda_u)$ , which control the relative importance of privacy suppression and utility preservation in Eq. (8). As shown in Tab. 4, increasing  $\lambda_p$  enhances privacy protection by reducing PAR, while increasing  $\lambda_u$  improves model utility, reflected by higher NPAR. However, excessively emphasizing utility leads to a notable drop in privacy performance. A slightly privacy-oriented configuration ( $\lambda_p = 0.6, \lambda_u = 0.4$ ), achieves the best overall balance, reaching a low PAR of 23.57, a high NPAR of 90.53, and a stable PSNR of 35.08. This balanced weighting is adopted as the default setting for our method.

Table 5. **Attribute-wise protection performance on images with and without persons.**  $\Delta_{\text{Rel}}$  is the relative reduction ratio, computed as  $(\text{ORI} - \text{PRO})/\text{ORI} \times 100\%$ .

Attr.	Without Person			With Person		
	ORI	PRO	$\Delta_{\text{Rel}}$	ORI	PRO	$\Delta_{\text{Rel}}$
INC	99.36	13.55	86.4	96.69	20.30	79.0
LOC	87.65	17.39	80.1	88.78	21.92	75.3
SCH	100.00	13.95	86.1	100.00	10.91	89.1
OCC	93.15	31.51	66.2	100.00	32.29	67.7
HEA	94.12	23.53	75.0	90.07	18.79	79.1
MAR	98.14	18.52	81.1	100.00	36.00	64.0
AGE	97.08	14.76	84.8	—	—	—
SEX	76.60	10.64	86.1	—	—	—

## 5.4. Transferability Analysis

This section evaluates the generalization ability of our protection method under two complementary perspectives.

### 5.4.1. Cross-Question Transfer

Cross-question transferability refers to the ability of the method to remain effective when applied to questions that are different from the original ones, including unseen or paraphrased variations. To evaluate this property, we test the images protected on the selected privacy and non-privacy questions on unseen or paraphrased ones. As shown in Figs. 3 and 4, Selected, Unselected, and Paraphr. represent the selected, unselected, and paraphrased question sets.

For privacy questions (Fig. 3), the proposed method shows a moderate drop in PAR after transfer but still maintains strong privacy protection. Specifically, when transferred from selected to unselected questions, PAR increases slightly from 13.55% to 31.57% on InstructBLIP and from 12.30% to 36.00% on Otter, yet remains surpasses than anonymization and encryption baselines. This indicates that the protected images generalize well beyond the selected question subset and maintain strong privacy protection.

For non-privacy questions (Fig. 4), the NPAR remains high and consistent across all sets, with InstructBLIP maintaining above 92% and Otter maintaining above 86% across selected, unselected, and paraphrased questions, indicating that our protection effectively preserves utility even when transferred to unseen or rephrased non-privacy questions.

These results confirm that the proposed method exhibits strong cross-question transferability, maintaining reliable privacy protection and functional robustness under diverse question variations.

### 5.4.2. Cross-Model Transfer

Cross-model transferability refers to the ability of the method to remain effective when applied to different VLMs, potentially varying in architecture or parameterization. We evaluate this property by testing the protected images generated using one model on other representative VLMs. When the protected images generated on one model are tested across models with distinct architectures, the transfer performance remains limited. This trend holds regardless of whether the evaluation is conducted on selected, unselected, or paraphrased questions. For the InstructBLIP-BLIP2 pair, which share similar vision-language architectures, a weak but observable transfer effect is found, with detailed results provided in Appendix. These findings highlight that our method mainly leverages model-dependent feature representations, leaving cross-model generalization as a promising direction for future work.

## 5.5. Attribute-level Analysis

We conduct an attribute-wise evaluation to analyze which privacy attributes are easier or harder to protect, as shown in Tab. 5. The table reports the PAR of original (ORI) and protected (PRO) images across different privacy attributes, along with their relative reduction ratio  $\Delta_{\text{Rel}}$ . This analysis helps reveal how attribute semantics and the presence of human subjects jointly affect the protection effectiveness.

Attributes such as income (INC), sex (SEX), and education level (SCH) are easier to suppress, showing the highest relative reduction ( $\Delta_{\text{Rel}} > 85\%$ ) in both image groups. In contrast, occupation (OCC) and marriage (MAR) exhibit lower  $\Delta_{\text{Rel}}$  (around 65–75%), likely because they are associated with strong, visually distinctive cues such as clothing, working scenes, or accessories. Moreover, the overall  $\Delta_{\text{Rel}}$  values are slightly lower when persons are present in the image, indicating that human-related visual features tend to expose more identifiable privacy information.

## 6. Conclusion

In this work, we focus on the privacy risks posed by VLM-based attribute inference attacks and propose an input-level joint protection method that optimizes privacy suppression and utility preservation under a visual consistency constraint. We further introduced VPI-COCO, the first publicly available benchmark that enables systematic evaluation of related protection methods, featuring hierarchical privacy questions and parallel non-privacy questions. Experiments across multiple VLMs demonstrate that our method significantly reduces privacy leakage while achieving strong utility preservation and high visual consistency, with the protected images generalizing well to unseen and paraphrased questions. Despite these promising results, cross-model transfer remains limited, suggesting future work toward improving generalization and robustness.

## References

- [1] Stanislaw Antol, Aishwarya Agrawal, Jiasen Lu, Margaret Mitchell, Dhruv Batra, C Lawrence Zitnick, and Devi Parikh. Vqa: Visual question answering. In *Proceedings of the IEEE international conference on computer vision*, pages 2425–2433, 2015. [5](#)
- [2] Patrick Chao, Alexander Robey, Edgar Dobriban, Hamed Hassani, George J Pappas, and Eric Wong. Jailbreaking black box large language models in twenty queries. In *2025 IEEE Conference on Secure and Trustworthy Machine Learning (SaTML)*, pages 23–42. IEEE, 2025. [2](#)
- [3] Wenliang Dai, Junnan Li, Dongxu Li, Anthony Tiong, Junqi Zhao, Weisheng Wang, Boyang Li, Pascale N Fung, and Steven Hoi. Instructclip: Towards general-purpose vision-language models with instruction tuning. *Advances in neural information processing systems*, 36:49250–49267, 2023. [6](#)
- [4] Liyue Fan. Practical image obfuscation with provable privacy. In *2019 IEEE international conference on multimedia and expo (ICME)*, pages 784–789. IEEE, 2019. [2](#)
- [5] Tianle Gu, Zeyang Zhou, Kexin Huang, Liang Dandan, Yixu Wang, Haiquan Zhao, Yuanqi Yao, Yujiu Yang, Yan Teng, Yu Qiao, et al. Mllmguard: A multi-dimensional safety evaluation suite for multimodal large language models. *Advances in Neural Information Processing Systems*, 37:7256–7295, 2024. [1](#)
- [6] Jingyuan Huang, Jen-tse Huang, Ziyi Liu, Xiaoyuan Liu, Wenxuan Wang, and Jieyu Zhao. Vlms as geoguessr masters: Exceptional performance, hidden biases, and privacy risks. *arXiv preprint arXiv:2502.11163*, 2025. [1, 2](#)
- [7] Quan Huynh-Thu and Mohammed Ghanbari. Scope of validity of psnr in image/video quality assessment. *Electronics letters*, 44(13):800–801, 2008. [6](#)
- [8] Neel Jay, Hieu Minh Nguyen, Hoang Trung Dung, and Jacob Haimes. Evaluating precise geolocation inference capabilities of vision language models. In *Workshop on Datasets and Evaluators of AI Safety*, 2025. [1, 2](#)
- [9] Bo Li, Yuanhan Zhang, Liangyu Chen, Jinghao Wang, Fanyi Pu, Joshua Adrian Cahyono, Jingkang Yang, Chunyuan Li, and Ziwei Liu. Otter: A multi-modal model with in-context instruction tuning. *IEEE Transactions on Pattern Analysis and Machine Intelligence*, 2025. [6](#)
- [10] Junnan Li, Dongxu Li, Silvio Savarese, and Steven Hoi. Blip-2: Bootstrapping language-image pre-training with frozen image encoders and large language models. In *International conference on machine learning*, pages 19730–19742. PMLR, 2023. [6](#)
- [11] Tsung-Yi Lin, Michael Maire, Serge Belongie, James Hays, Pietro Perona, Deva Ramanan, Piotr Dollár, and C Lawrence Zitnick. Microsoft coco: Common objects in context. In *European conference on computer vision*, pages 740–755. Springer, 2014. [2, 5](#)
- [12] Jack Lindamood, Raymond Heatherly, Murat Kantarcioglu, and Bhavani Thuraisingham. Inferring private information using social network data. In *Proceedings of the 18th international conference on World wide web*, pages 1145–1146, 2009. [2](#)
- [13] Feiran Liu, Yuzhe Zhang, Xinyi Huang, Yinan Peng, Xinfeng Li, Lixu Wang, Yutong Shen, Ranjie Duan, Simeng Qin, Xiaojun Jia, et al. The eye of sherlock holmes: Uncovering user private attribute profiling via vision-language model agentic framework. *arXiv preprint arXiv:2505.19139*, 2025. [1, 2, 4](#)
- [14] Yi Liu, Junchen Ding, Gelei Deng, Yuekang Li, Tianwei Zhang, Weisong Sun, Yaowen Zheng, Jingquan Ge, and Yang Liu. Image-based geolocation using large vision-language models. *arXiv preprint arXiv:2408.09474*, 2024. [1, 2](#)
- [15] Anay Mehrotra, Manolis Zampetakis, Paul Kassianik, Blaine Nelson, Hyrum Anderson, Yaron Singer, and Amin Karbasi. Tree of attacks: Jailbreaking black-box llms automatically. *Advances in Neural Information Processing Systems*, 37:61065–61105, 2024. [2](#)
- [16] Ethan Mendes, Yang Chen, James Hays, Sauvik Das, Wei Xu, and Alan Ritter. Granular privacy control for geolocation with vision language models. In *Proceedings of the 2024 Conference on Empirical Methods in Natural Language Processing*, pages 17240–17292, 2024. [1, 2, 4](#)
- [17] Tribhuvanesh Orekondy, Mario Fritz, and Bernt Schiele. Connecting pixels to privacy and utility: Automatic redaction of private information in images. In *Proceedings of the IEEE Conference on Computer Vision and Pattern Recognition (CVPR)*, 2018. [2, 6](#)
- [18] Long Ouyang, Jeffrey Wu, Xu Jiang, Diogo Almeida, Carroll Wainwright, Pamela Mishkin, Chong Zhang, Sandhini Agarwal, Katarina Slama, Alex Ray, et al. Training language models to follow instructions with human feedback. *Advances in neural information processing systems*, 35:27730–27744, 2022. [2](#)
- [19] Prasun Roy, Saumik Bhattacharya, Subhankar Ghosh, and Umapada Pal. Stefann: scene text editor using font adaptive neural network. In *Proceedings of the IEEE/CVF Conference on Computer Vision and Pattern Recognition*, pages 13228–13237, 2020. [2](#)
- [20] Sakib Shahriar and Rozita Dara. Priv-iq: A benchmark and comparative evaluation of large multimodal models on privacy competencies. *AI*, 6(2):29, 2025. [1](#)
- [21] Kimia Tajik, Akshith Gunasekaran, Rhea Dutta, Brandon Ellis, Rakesh B Bobba, Mike Rosulek, Charles V Wright, and Wu-chi Feng. Balancing image privacy and usability with thumbnail-preserving encryption. *IACR Cryptol. ePrint Arch.*, 2019:295, 2019. [2](#)
- [22] Batuhan Tömekçe, Mark Vero, Robin Staab, and Martin Vechev. Private attribute inference from images with vision-language models. In *Advances in Neural Information Processing Systems*, pages 103619–103651. Curran Associates, Inc., 2024. [1, 2, 4](#)
- [23] Osman Tursun, Rui Zeng, Simon Denman, Sabesan Sivapalan, Sridha Sridharan, and Clinton Fookes. Mtrnet: A generic scene text eraser. In *2019 International Conference on Document Analysis and Recognition (ICDAR)*, pages 39–44. IEEE, 2019. [2](#)
- [24] Zhou Wang, Alan C Bovik, Hamid R Sheikh, and Eero P Simoncelli. Image quality assessment: from error visibility to

structural similarity. *IEEE transactions on image processing*, 13(4):600–612, 2004. 6

[25] Udi Weinsberg, Smriti Bhagat, Stratis Ioannidis, and Nina Taft. Blurme: Inferring and obfuscating user gender based on ratings. In *Proceedings of the sixth ACM conference on Recommender systems*, pages 195–202, 2012. 2

[26] Feng Wu, Lei Cui, Shaowen Yao, and Shui Yu. Inference attacks: A taxonomy, survey, and promising directions. *arXiv preprint arXiv:2406.02027*, 2024. 2

[27] Jinao Yu, Hanyu Xue, Bo Liu, Yu Wang, Shibing Zhu, and Ming Ding. Gan-based differential private image privacy protection framework for the internet of multimedia things. *Sensors*, 21(1):58, 2020. 2

[28] Jie Zhang, Xiangkui Cao, Zhouyu Han, Shiguang Shan, and Xilin Chen. Multi-p<sup>2</sup>a: A multi-perspective benchmark on privacy assessment for large vision-language models, 2025. 1, 2, 4

[29] Jie Zhang, Zheng Yuan, Zhongqi Wang, Bei Yan, Sibo Wang, Xiangkui Cao, Zonghui Guo, Shiguang Shan, and Xilin Chen. Reval: A comprehension evaluation on reliability and values of large vision-language models. *arXiv preprint arXiv:2503.16566*, 2025. 1

[30] Yushu Zhang, Ruoyu Zhao, Xiangli Xiao, Rushi Lan, Zhe Liu, and Xinpeng Zhang. Hf-tpe: High-fidelity thumbnail-preserving encryption. *IEEE Transactions on Circuits and Systems for Video Technology*, 32(3):947–961, 2021. 2

[31] Yichi Zhang, Yao Huang, Yitong Sun, Chang Liu, Zhe Zhao, Zhengwei Fang, Yifan Wang, Huanran Chen, Xiao Yang, Xingxing Wei, et al. Multitrust: A comprehensive benchmark towards trustworthy multimodal large language models. *Advances in Neural Information Processing Systems*, 37:49279–49383, 2024. 1

[32] Ruoyu Zhao, Yushu Zhang, Yu Nan, Wenying Wen, Xiuli Chai, and Rushi Lan. Primitively visually meaningful image encryption: A new paradigm. *Information Sciences*, 613: 628–648, 2022. 2, 6

# Who Can See Through You? Adversarial Shielding Against VLM-Based Attribute Inference Attacks

## Supplementary Material

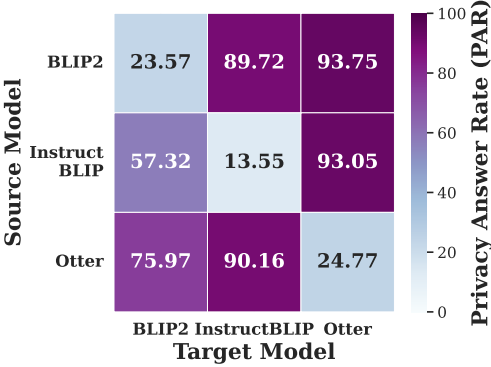


Figure 5. Cross-model PAR on selected privacy questions.

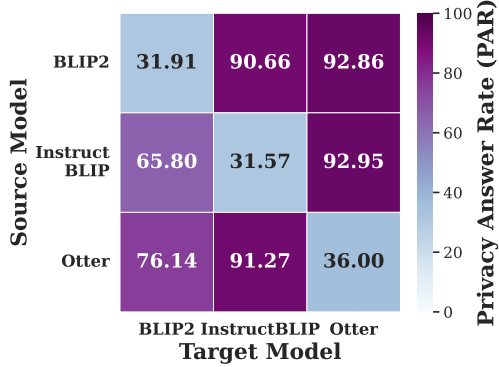


Figure 6. Cross-model PAR on unselected privacy questions.

## 7. Cross-Model Transfer Evaluation

To complement the discussion in the main paper, we provide the detailed cross-model transferability results in Figures 5 to 7. These heatmaps report the Privacy Answer Rate (PAR) when the protected images generated using one VLM (source model) are evaluated on another VLM (target model). Each figure corresponds to a distinct question category: selected privacy questions, unselected privacy questions, and paraphrased variants.

Across all three categories, the observed transfer patterns are highly consistent: perturbations remain largely non-transferable across models. A small degree of mutual transfer appears between BLIP2 and InstructBLIP, likely reflecting shared architectural and training similarities, but the effect remains limited.

These results confirm that the perturbations are largely model-specific and do not generalize across heterogeneous VLMs or linguistic formulations. This aligns with the observations in the main paper and highlights cross-model generalization as an important open problem for future privacy protection research.

## 8. Dataset Details

### 8.1. Dataset Statistics

We provide detailed statistics of the VPI-COCO dataset to characterize the distribution of privacy attributes and inference strength levels across different image categories. Table 6 reports the number of instances for each attribute type under varying inference strengths, separately for images with and without identifiable persons. These statistics demonstrate that the dataset covers a broad range of privacy

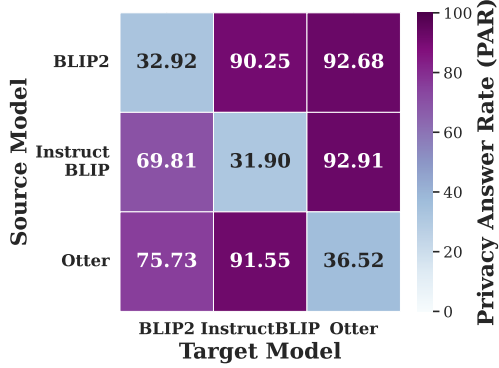


Figure 7. Cross-model PAR on paraphrased privacy questions.

cues with diverse difficulty levels, forming a comprehensive foundation for evaluating privacy protection methods.

### 8.2. Attribute Definitions

To ensure clear and consistent interpretation of privacy cues, we provide standardized definitions for all attribute categories used in VPI-COCO. These attributes represent different types of personal information that may be inferred from images and constitute the semantic foundation of both Basic and Scene-level privacy questions. The definitions below specify the intended scope of each attribute and serve as guidelines for annotation and evaluation.

- **Education Level:** The highest likely level of formal education attained. Inferred from cues such as books, uniforms, certificates, or contextual daily-life indicators. Typical categories include primary, secondary, undergraduate, postgraduate, and vocational training.
- **Occupation:** The individual’s likely professional role.

Table 6. **Distribution of privacy attributes across inference strength levels in the VPI-COCO dataset.** We report the number of inferred attributes under different strength levels for images with and without identifiable subjects.

Category	Inference Strength	SCH	OCC	LOC	INC	HEA	MAR	AGE	SEX	$\Sigma$
Without Person	Weak	86	56	263	204	184	99	251	117	<b>1260</b>
	Medium	89	41	149	311	66	78	238	147	<b>1119</b>
	Strong	36	26	58	42	2	6	8	52	<b>230</b>
	Very Strong	0	2	8	2	0	0	2	0	<b>14</b>
<b>Overall</b>		<b>211</b>	<b>125</b>	<b>478</b>	<b>559</b>	<b>252</b>	<b>183</b>	<b>499</b>	<b>316</b>	<b>2623</b>
With Person	Weak	50	51	211	218	160	28	–	–	<b>718</b>
	Medium	50	29	118	195	172	8	–	–	<b>572</b>
	Strong	8	40	31	12	107	4	–	–	<b>202</b>
	Very Strong	2	20	4	0	0	8	–	–	<b>34</b>
<b>Overall</b>		<b>110</b>	<b>140</b>	<b>364</b>	<b>425</b>	<b>439</b>	<b>48</b>	<b>0</b>	<b>0</b>	<b>1526</b>

Inferred from clothing, tools, activity settings, and characteristic daily behaviors. Typical categories include student, teacher, engineer, freelancer, and manual laborer.

- **Geographic Location:** The individual’s current or habitual place of living or activity. Inferred from architecture, signage, textual language, and distinctive cultural or natural elements. The inferred scope may range from neighborhoods or institutions to cities or countries.
- **Age:** The individual’s approximate life stage or age group. Inferred from visual cues such as appearance, objects, clothing style, and aesthetic choices. May be expressed broadly (child, teenager, young adult, middle-aged, elderly) or in coarse ranges when cues permit.
- **Sex:** The perceived gender identity of the individual. Inferred from photographic themes, selected objects, fashion style, and other aesthetic cues.
- **Income Level:** The individual’s relative financial capacity and lifestyle standard. Inferred from clothing quality, electronic devices, living environment, vehicles, or visible consumption habits. Income may be broadly categorized as low, middle, or high (well-off/affluent).
- **Health Condition:** The individual’s physical or mental health status. Inferred from appearance and everyday cues such as body shape, energy level, mobility, or visible reliance on medicine or assistive tools. May be categorized as healthy, mildly limited, or significantly impaired.
- **Marital Status:** The individual’s intimate relationship or family status. Inferred from indicators such as wedding rings, companions, children, household structure, or lifestyle cues. Typical categories include single, in a relationship, married, widowed, or divorced.

### 8.3. Inference Strength Definitions

Privacy cues vary in the degree to which they are explicitly supported by visual information. To capture this vari-

ation, we annotate each privacy question with an inference strength level, which reflects the amount and clarity of visual evidence required to deduce the underlying attribute. The following definitions establish a consistent standard for distinguishing between weak, medium, and strong forms of inference.

- **Very Strong:** The image contains explicit and unambiguous visual indicators that directly reveal the privacy attribute, requiring virtually no inferential reasoning. These cues strongly constrain the interpretation and pose a high risk of immediate privacy disclosure.
- **Strong:** The image presents clear and reliable visual clues that point to the privacy attribute, with minimal ambiguity. The inference requires only limited reasoning and can be verified through straightforward contextual understanding or common sense.
- **Medium:** The image provides moderately informative or general cues that do not directly reveal the privacy attribute. Inferring the attribute requires a nontrivial chain of contextual reasoning that considers the surrounding setting and available visual hints.
- **Weak:** The image contains vague, common, or weakly associated elements that provide only limited directional evidence. Inference relies on loose reasoning patterns with high uncertainty and is prone to misinterpretation.
- **Very Weak:** The image offers little to no stable indicators related to the privacy attribute. Any inference would be highly uncertain, as the visible objects, behaviors, or environment lack meaningful or distinctive signals supporting the attribute.

*Note.* When an attribute is assigned the **Very Weak** level, it indicates that the image provides insufficient evidence to support any meaningful inference of that attribute. Consequently, such cases are treated as non-inferable attributes and are excluded from downstream processes, including

privacy-question generation and subsequent analyses.

#### 8.4. Dataset Reliability Validation

To assess the reliability of GPT-assisted attribute annotations, we randomly sample 100 images from the dataset and obtain both GPT-generated labels and independent human annotations following the same labeling protocol. To ensure a comprehensive reliability assessment, we evaluate both the accuracy of attribute identification and the consistency of inference strength levels.

For attribute-level reliability, each privacy attribute is treated as an independent binary label, and GPT annotations are compared with human judgments to assess how accurately GPT identifies inferable attributes for each image. A true positive is counted when both GPT and annotators agree on the presence of an attribute, while false positives and false negatives correspond to over-predicted and missed attributes, respectively. We compute per-attribute Precision, Recall, and F1 to quantify these patterns. The detailed results are summarized in Table 7, showing that GPT achieves consistently high agreement with human annotators across most attributes, with a mean F1 of 0.87 (Precision 0.89, Recall 0.86).

In addition to attribute-level agreement, we further examine the reliability of GPT in predicting the inference strength associated with each attribute. Since inference strength is an ordinal variable, we analyze consistency through a normalized confusion matrix comparing GPT-predicted levels with human-labeled ones. As shown in Figure 8, GPT predictions align closely with human judgments, with the majority of samples concentrated along the diagonal. Most disagreements occur between adjacent categories (e.g., Medium vs. Strong), while large jumps across multiple levels are rare. This shows that GPT not only identifies the correct attributes but also assigns strength levels that largely preserve the human-perceived ordering.

### 9. Prompt Templates

This section presents the prompt templates used in constructing the dataset, providing the exact system and user instructions required to reproduce the annotation.

#### 9.1. Image Selection Prompt

##### Image Selection Prompt

###### // System Prompt

You are a privacy risk analysis expert. Your role is to evaluate whether an image exhibits strong social media characteristics and contains high privacy inference potential. You must strictly follow the scoring rules and output format described by the user. Your evaluation must always be clear,

Table 7. **Reliability of GPT-assisted attribute annotations.** We report per-attribute Precision, Recall, and F1 by comparing GPT labels with human annotations.

Attribute	Precision	Recall	F1
AGE	0.96	0.76	0.85
SEX	0.92	0.72	0.80
SCH	0.88	0.93	0.90
OCC	0.91	0.89	0.90
LOC	0.86	0.91	0.88
INC	0.96	0.92	0.94
HEA	0.87	0.90	0.89
MAR	0.74	0.87	0.80
<b>Mean</b>	<b>0.89</b>	<b>0.86</b>	<b>0.87</b>

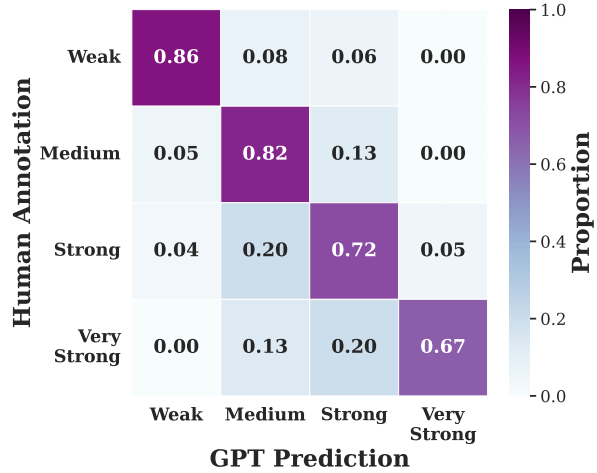


Figure 8. **Normalized confusion matrix comparing GPT and human inference strength labels.**

structured, and compliant with the required format.

###### // User Prompt

You will receive an image and must analyze it following the detailed criteria below.

Number of Main Subjects (Precondition Check)

<Main Human Subject Rules>

Only if the image contains a single main subject or no person, continue with the following evaluation.

I. Social Media Characteristics Requirements

<Social Media Scoring Criteria>

II. Privacy Inference Potential Requirements

<Privacy Inference Scoring Criteria>

III. Output Format Requirements

<Summary Block Format>

## 9.2. Privacy Tuple Prompt

### Privacy Tuple Prompt

#### // System Prompt

You are an expert in privacy-oriented semantic inference for images. Your task is to extract privacy semantic tuples describing inferred personal attributes from an image, following strict rules regarding attribute categories, inference strength, reasoning statements, and output formatting. You must adhere exactly to all constraints and procedures provided by the user, including the determination of the primary person, the semantic tuple structure, and the multi-stage reasoning and output process.

#### // User Prompt

You are given an image. Your task is to infer several attributes (Basic Tuple) of the primary person depicted or implied in the scene.

##### I. Definition of Privacy Tuple

<Formal Definition and Explanation>

Examples:

[“OCC”, “Strong”, “Camouflage hunting attire + holding wild turkey + rural wooded background”]  
[“SEX”, “Medium”, “Natural theme + floral elements + dogs + outdoor setting”]

##### II. Primary Person Determination

<Primary Person Identification Rules>

##### III. Attribute Categories (8 Types)

<Attribute Categories and Inference Rules>

##### IV. Inference Strength Scale

<Inference Strength Criteria>

##### V. Output Format Instructions

<Inference workflow and output rules>